ELSEVIER

Journal of Chromatography A, 877 (2000) 25–39

JOURNAL OF CHROMATOGRAPHY A

www.elsevier.com/locate/chroma

Characterization of C_{18}-bonded liquid chromatographic stationary phases by Raman spectroscopy: the effect of mobile phase composition

Charles A. Doyle[a], Thomas J. Vickers[b], Charles K. Mann[b], John G. Dorsey[b,*]

[a]*Department of Chemistry, University of Cincinnati, Cincinnati, OH 45221-0172, USA*

[b]*Department of Chemistry, Florida State University, Tallahassee, FL 32306-4390, USA*

Received 2 June 1998; received in revised form 25 November 1999; accepted 29 December 1999

Abstract

Raman spectroscopy is used to examine the effect of mobile phase composition on the orientation of octadecyl-bonded silica-based reversed-phase liquid chromatographic (RPLC) stationary phase ligands. The effect of ligand bonding density is also investigated. The present experimental set-up utilizes a direct, noninvasive, on-column approach to examine the solvent dependent conformational behavior of the bonded ligands under flow-rate and back pressure conditions similar to those used during conventional RPLC measurements. Neat, single-component, mobile phase solvents including water, acetonitrile, methanol and chloroform are used to investigate the hypothesized collapsing and extension of stationary phase ligands with changes in mobile phase composition. No evidence of phase collapse was observed upon changing the mobile phase composition from an organic to an aqueous content. Also, Raman spectroscopic measurements allowed the differentiation between associated and free acetonitrile solvent.

Keywords: Stationary phases, LC; Raman spectroscopy; Mobile phase composition

1. Introduction

Although there has been much recent effort focused on preparing novel stationary phases such as alumina-, zirconia- and titania-based phases, a variety of polymer-based materials, polymer-coated metal oxides and unique bonded ligands [1], conventional octyl and octadecyl bonded silica-based stationary phases are still the most widely used, and the most extensively characterized reversed-phase liquid chromatographic (RPLC) stationary phase materials. The role of the stationary phase in liquid chromatographic separations has received considerable theoretical and experimental attention. Initial theoretical descriptions of the retention process treated bonded alkyl ligands of the stationary phase as passive receptors of nonpolar solute molecules that were expelled from the polar mobile phases typically employed in reversed-phase liquid chromatography [2–5]. In contrast, a number of studies have shown that the bonded stationary phase ligands take a more active role in the retention process. Retention and selectivity have both been shown to be affected by the type of bonding chemistry, or the functionality (monomeric versus polymeric), of the stationary phase [6–14]; the chain length of the bonded alkyl

*Corresponding author. Tel.: +1-850-644-4496; fax: +1-850-645-5644.

E-mail address: dorsey@chem.fsu.edu (J.G. Dorsey)

0021-9673/00/$ – see front matter
PII: S0021-9673(00)00175-8

ligands [15–21]; and the number of alkyl ligands attached to the support surface per unit area (ligand bonding density) [13,19,20,22].

In addition to changes in solute retention based upon the above-mentioned differences in the physical constitution of different stationary phase ligands, changes in solute retention have also been attributed to conformational changes of the bonded alkyl ligands for a given stationary phase. Changes in solute retention with changes in the composition of hydro–organic mobile phases reflect these conformational changes of the bonded ligands [23–35]. The solvent-induced conformational changes of the bonded ligands have also been investigated by a variety of other analytical methods in addition to chromatographic studies including: nuclear magnetic resonance [36,37], fluorescence [38], optical transmittance [35] and vibrational [39–41] spectroscopic techniques. The bonded alkyl chains of the stationary phase are hypothesized to extend away from the support surface in a 'brush-like' configuration in the presence of nonpolar solvents, and to collapse toward the support surface in relatively polar mobile phases.

Yonker et al. [28,29] envisioned the 'freezing' of bonded alkyl chains (C_8 or C_{18}), due to intra- and/or intermolecular bonded chain interactions, as causing the entrapment of water in a 'tent' of alkyl chains to account for the observation that excess water was associated with the stationary phase ligands in 100% water mobile phases. Further, for C_{18} ligands [28], they envisioned that increasing the methanol content of the water–methanol mobile phase mixture unzipped the intermolecular bonded-chain interactions from top to bottom (from the distal carbon down to the point of surface attachment) of the alkyl chain until, with continued increases in methanol content, the bonded chains become more 'erect' and 'brush'-like. Martire and Boehm [30] considered the alkyl bonded stationary phase as a 'breathing' surface in which the alkyl chains become 'swollen' by solvent penetration and are extended away from the support surface in the presence of nonpolar solvents, but collapse upon one another and toward the support surface in the presence of more polar solvents so as to continually maintain a relatively nonpolar surface character.

In contrast, the molecular dynamics simulations of Klatte and Beck [42,43] indicate that for water–methanol mobile phases with volume ratios less than 80–90% methanol, methanol wets the interfacial surface of the stationary phase but does not appreciably alter the structure of the C_{18} chains. These simulation results are also in agreement with the frequency-domain fluorescence anisotropy measurements of Montgomery et al. [44] for low organic content aqueous–alcohol mobile phase mixtures.

The present investigation is using a direct, noninvasive, on-column approach to examine the solvent-dependent conformational behavior of bonded C_{18} ligands under flowing conditions by Raman spectroscopy. The neat mobile phases used in this study include: water, acetonitrile, methanol and chloroform. The relative polarity (P') of these mobile phases varies from $P'=10.2$ for the polar solvent water to $P'=4.1$ for chloroform, where the nonpolar solvent *n*-pentane is assigned $P'=0.0$ [45]. In addition, the bonded chain rigidity is also being investigated by examining two stationary phases differing only in ligand bonding density: a 2.34 and a 3.52 μmol m^{-2} Microporasil C_{18} stationary phase.

2. Experimental

2.1. Instrumentation

The Raman spectroscopy – liquid chromatography (Raman–LC) experimental set-up has been previously described [46]. Custom-built stainless steel Raman–LC columns, each adapted with a quartz optical viewing window positioned normal to the direction of mobile phase flow, allow the stationary phases to be packed using conventional high-performance liquid chromatographic (HPLC) column slurry packing procedures and to be examined spectroscopically at typical LC mobile phase flow-rates and back pressures. Mobile phases were pumped through the Raman–LC columns at 1.0 ml min^{-1} using a Spectra-Physics SP8800 ternary HPLC pump (ThermoSeparations, San Jose, CA, USA) and the columns were thermostatted to within ± 0.1 °C of the desired temperature (35°C for this work) using a Fisher model 9100 isotemp refrigerated circulator (Fisher Scientific, Atlanta, GA, USA). A thermostatted liquid–solid cell with a design similar to the

Raman LC columns [46] was used for static solvent measurements.

The Raman spectroscopic portion of the experimental set-up [46–48] consists of a dispersive Raman spectrometer equipped with a fiber optic probe. The excitation radiation (514.5 nm) from an argon ion laser (Stabilite 2017 with a 2550 Controller; Spectra-Physics, Mountain View, CA, USA) operating at a power of 150 mW at the fiber tip, is directed through the quartz optical viewing window of the Raman–LC column and into the mobile phase/stationary phase sample matrix by a 400-μm diameter core all silica optical fiber. The second fiber of the bifurcated fiber-optic probe collects the scattered radiation and directs it to the entrance optics of a Jobin Yvon HR640 spectrograph (Instruments SA, Edison, NJ, USA), where the radiation is then dispersed by a grating onto an 1152×298 pixel liquid nitrogen-cooled charge coupled device (CCD) detector (Princeton Instruments, Trenton, NJ, USA). A spectrograph entrance slit width of 300 μm and a 1200 grooves/mm grating are used for the C–C stretching and C–H bending spectral region, whereas a 200-μm slit width and a 600 grooves/mm grating are used for the C–H stretching region. All 298 pixels of the CCD are binned in the direction parallel to slit height. The collected signals are digitized and transferred to an IBM compatible personal computer, which also controls data collection, for data treatment using custom-developed software.

2.2. Stationary phases and reagents

The stationary phases investigated were synthesized 'in house' from commercially available Microporasil starting silica (Waters, Milford, MA, USA) and monofunctional octadecyldimethylchlorosilane (United Chemical Technologies, Bristol, PA, USA) using established reflux and ultrasound synthetic procedures [49,50]. The Microporasil starting silica consisted of irregularly shaped 6–10 μm particles with 125 Å pores to give a total surface area of 311 m^2 g^{-1}. Monofunctional octadecyl ligand bonding densities of 2.34 and 3.52 μmol m^{-2} were achieved, as calculated from the surface area of the starting silica and the percentage of carbon as determined by elemental analysis.

The stationary phases were packed into individual Raman–LC columns by slurry packing techniques using an air-driven pump (Alltech Associates, Deerfield, IL, USA). Following column packing, the stationary phases were equilibrated by passing at least 500 ml of 100% acetonitrile through each column, then gradually changing the mobile phase composition from 100% acetonitrile to 100% water over about a 6-h time period (at a flow-rate of 1 ml min^{-1}), and finally equilibrating the stationary phases with at least 1 l of water at a flow–rate of 1 ml min^{-1} before performing the spectroscopic investigations. HPLC grade acetonitrile, methanol and chloroform (Fisher, Atlanta, GA, USA) and distilled water which had been further purified by passage through a Barnstead Nanopure II water purification system (Barnstead, Newton, MA, USA) equipped with a 0.45-μm filter, were used as equilibrating and mobile phase solvents. The relative polarities (P') of these mobile phase solvents decrease from a value of $P'=10.2$ for water, $P'=5.8$ for acetonitrile, $P'=5.1$ for methanol, to a value of $P'=4.1$ for chloroform [45]. Similar mobile phase composition changing procedures were employed to equilibrate the stationary phases with each of the individual solvents. The stationary phases were thermostatted at 35°C for at least 1 h, while pumping the appropriate solvent through the column, prior to spectroscopic measurements.

3. Results and discussion

3.1. Subtraction of mobile phase features

The neat mobile phase Raman spectroscopic features, and their removal from the features due to the ligands of the 3.52 μmol m^{-2} Microporasil C_{18} stationary phase in the presence of the respective solvents, are presented for water (H_2O), acetonitrile (ACN), methanol (MeOH), and chloroform ($CHCl_3$) in Figs. 1, 2, 3, and 4, respectively. It should be noted that the spectral features of the solvents are independent of whether or not the liquids are flowing or static. However, solvent spectral features are sensitive to the liquid's molecular environment. Exposure times were varied from 2 to 20 s so as to provide about 80% of the detector's maximum signal response. Signals were co-added to give total data

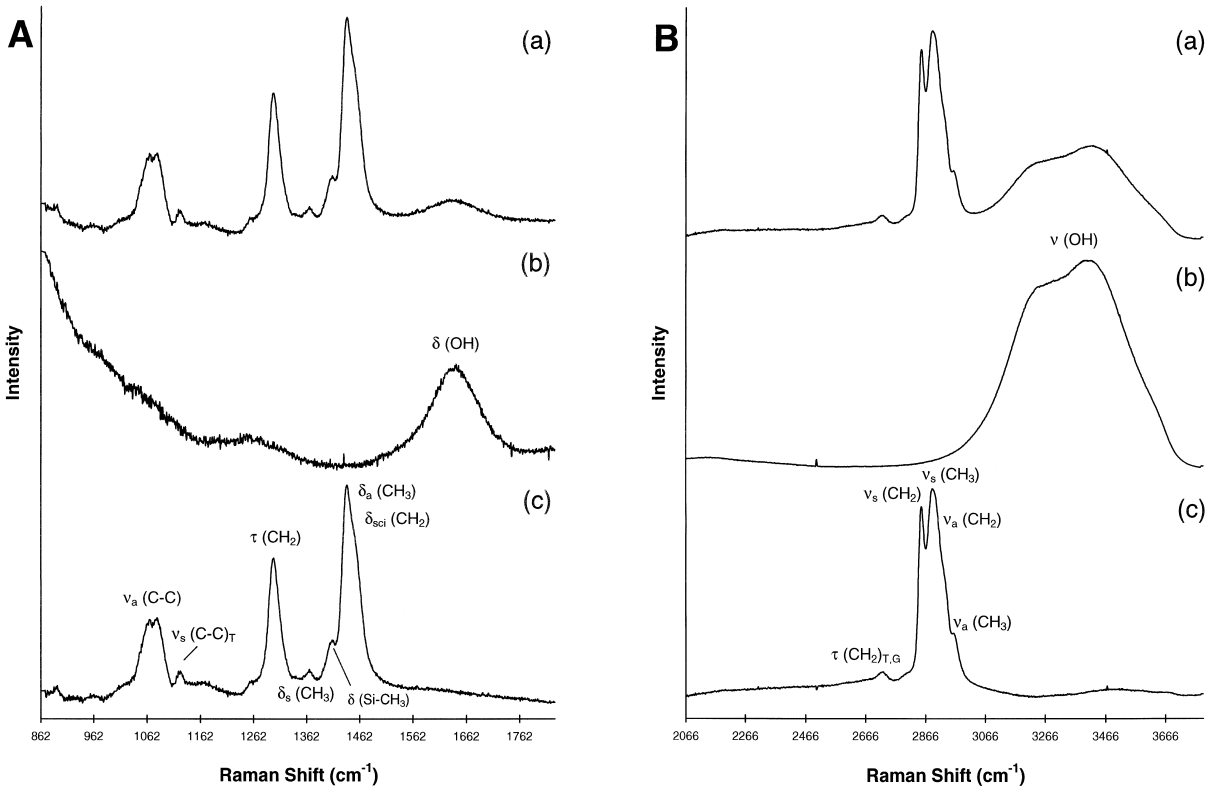

Fig. 1. (A) Comparison of the spectral features in the C–C stretching and C–H bending region due to the bonded ligands of the 3.52 μmol m^{-2} Microporasil C_{18} stationary phase at 35°C (a) in the presence and (c) absence of the spectral features due to the (b) water mobile phase (1.0 ml min^{-1}). The spectra have been multiplied by the following scaling factors: (a) ×1.014, (b) ×2.024, (c) ×1. (B) Same as (A), except that the spectral region is the C–H stretching region. Spectral scaling factors: (a) ×1.267, (b) ×1, (c) ×1.273.

acquisition times of 4 min for all stationary phases packed in the Raman–LC columns and 2 min for all static liquid measurements. Triplicate measurements were performed under each stationary phase–mobile phase–temperature combination of conditions and yielded comparable results. For all spectra in this article, the features due to the fiber-optic probe [46] have already been subtracted. Interactive spectral subtraction [46,51] involves the removal of pure component reference spectral features from the spectral features of a complex matrix such that any additional subtraction would introduce 'negative-going' or 'derivative-like' features in the remaining spectral features of the matrix.

3.1.1. Subtraction of water features

The spectroscopic features of the 3.52 μmol m^{-2} Microporasil C_{18} stationary phase ligands at 35°C in the presence of the features due to the neat water mobile phase are presented in spectrum a of Fig. 1 for both the carbon–carbon stretching (C–C stretching) and the carbon– hydrogen bending (C–H bending) region (low wavenumber region) (Fig. 1A) and the carbon– hydrogen stretching (C–H stretching) region (high wavenumber region) (Fig. 1B). The features due to neat H_2O at 35°C are presented in spectrum b of Fig. 1. The results of the subtraction of spectral features due to H_2O (spectrum b) from the spectrum of the C_{18} bonded ligands in the presence of the H_2O mobile phase (spectrum a) to give the spectral features due only to the C_{18} stationary phase ligands are shown in spectrum c of Fig. 1.

As discussed previously [46], water is a convenient solvent spectroscopically, because the features due to oxygen–hydrogen bending [δ (OH)] at 1640 cm^{-1} and oxygen–hydrogen stretching [ν (OH)] in

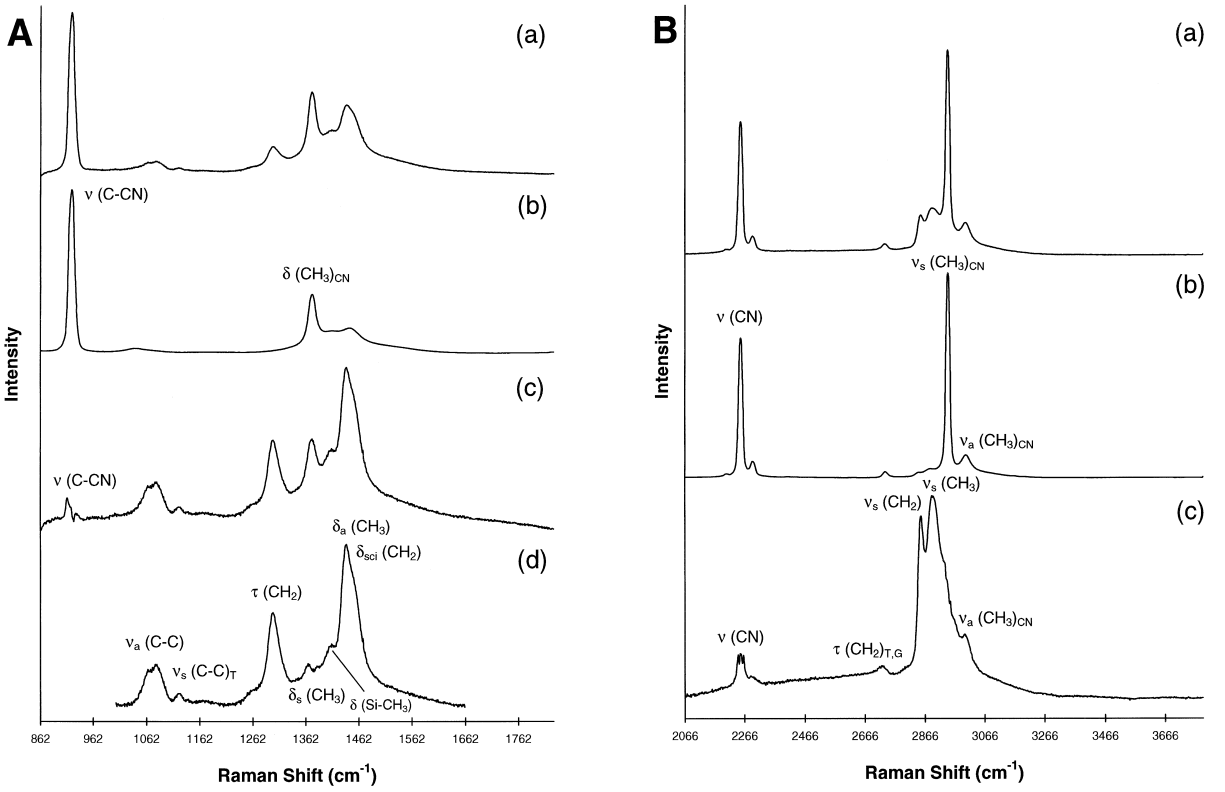

Fig. 2. (A) Comparison of the spectral features in the C–C stretching and C–H bending region due to the bonded ligands of the 3.52 μmol m^{-2} Microporasil C_{18} stationary phase at 35°C (a) in the presence of (c) after partial removal of and (d) in the absence of the spectral features due to the (b) acetonitrile mobile phase (1.0 ml min^{-1}). Spectral scaling factors: (a) ×2.803, (b) ×1, (c) ×9.904, (d) ×12.32. (B) Comparison of the spectral features in the C–H stretching region due to the bonded ligands of the 3.52 μmol m^{-2} Microporasil C_{18} stationary phase at 35°C (a) in the presence and (c) absence of the spectral features due to the (b) acetonitrile mobile phase (1.0 ml min^{-1}). Spectral scaling factors: (a) ×3.394, (b) ×1, (c) ×17.67.

the range from about 2850 to 3750 cm^{-1}, are readily subtracted from the hydrocarbon features of the 3.52 μmol m^{-2} C_{18} stationary phase ligands. Thus, the hydrocarbon features of the C_{18} stationary phase ligands (spectrum c) are readily observable in the presence of the H_2O mobile phase (spectrum a). Characteristic bands [41,46,52,53] of the octadecylsilyl stationary phase ligands due to carbon–carbon asymmetric stretching [ν_a (C–C)] in the region from about 1030 to 1110 cm^{-1}; carbon–carbon symmetric stretching [ν_s $(C–C)_T$] of the alkyl chains in the *trans* conformation at 1123 cm^{-1}; methylene in-phase twisting [τ (CH_2)] at 1299 cm^{-1}; methyl symmetric bending [δ_s (CH_3)] at 1367 cm^{-1}; methyl–silicon deformations [δ $(Si–CH_3)$] at 1410 cm^{-1}; and to a combination of methyl asymmetric bending [δ_a (CH_3)] and methylene scissoring [δ_{sci} (CH_2)] at 1437 cm^{-1} are present in the low wavenumber region (Fig. 1A). Bands due to methylene twisting [τ $(CH_2)_{T,G}$] at 2722 cm^{-1}, methylene symmetric stretching [ν_s (CH_2)] at 2852 cm^{-1}, methyl symmetric stretching [ν_s (CH_3)] at 2890 cm^{-1}, methylene asymmetric stretching [ν_a (CH_2)] at roughly 2923 cm^{-1} and methyl asymmetric stretching [ν_a (CH_3)] at 2960 cm^{-1} are present in the high wavenumber region (Fig. 1B).

3.1.2. Subtraction of acetonitrile features

The spectroscopic features due to the combination of the acetonitrile mobile phase and the ligands of the 3.52 μmol m^{-2} C_{18} phase at 35°C are presented

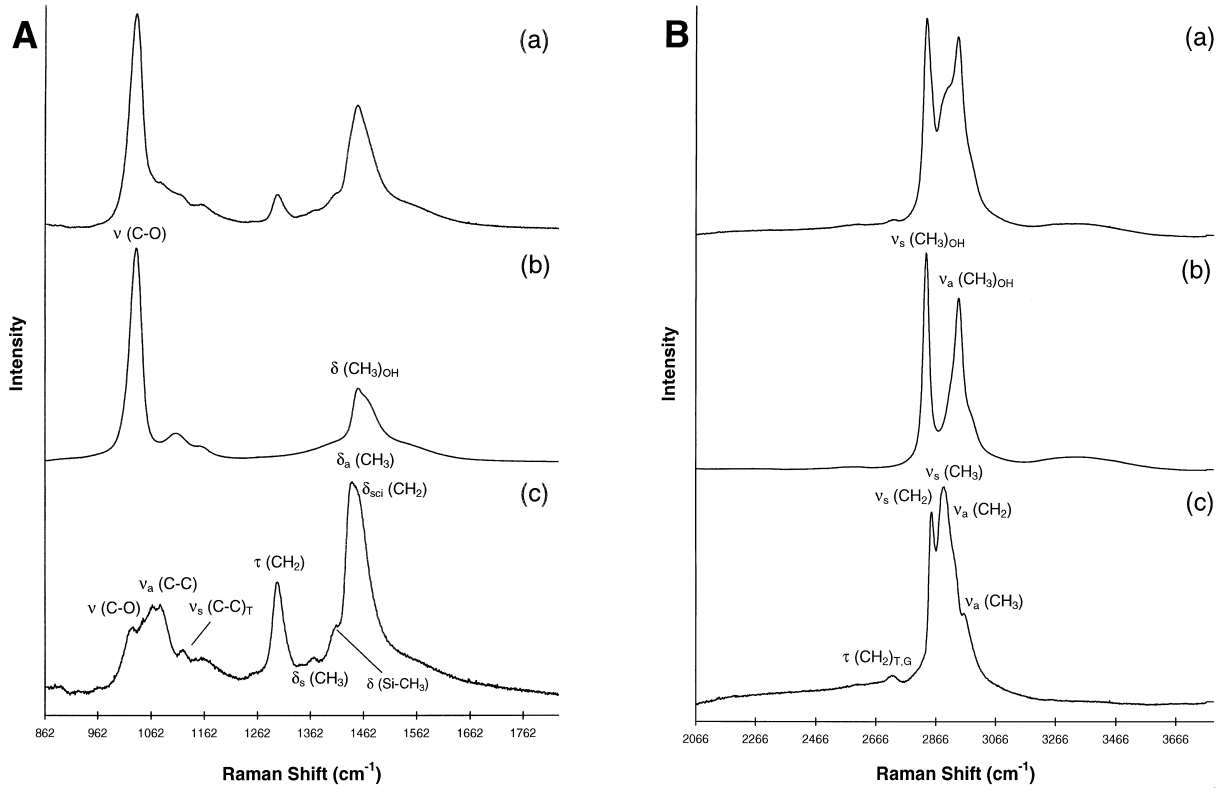

Fig. 3. (A) Comparison of the spectral features in the C–C stretching and C–H bending region due to the bonded ligands of the 3.52 μmol m^{-2} Microporasil C_{18} stationary phase at 35°C (a) in the presence and (c) after partial removal of the spectral features due to the (b) methanol mobile phase (1.0 ml min^{-1}). Spectral scaling factors: (a) ×3.055, (b) ×1, (c) ×10.32. (B) Same as (A), except that the spectral region is the C–H stretching region. Spectral scaling factors: (a) ×3.099, (b) ×1, (c) ×6.862.

in spectrum a, and the neat ACN features are shown in spectrum b of Fig. 2. In the low wavenumber region (Fig. 2A), ACN spectral features due to carbon–nitrile stretching [ν (C–CN)] at 921 cm^{-1} and to deformations of the nitrile-bonded methyl group [δ $(CH_3)_{CN}$] at 1374 cm^{-1} are the most prominent features in spectrum a, although the τ (CH_2) and δ_a $(CH_3)/\delta_{sci}$ (CH_2) bands due to the bonded octadecyl ligands are also evident.

Spectrum c of Fig. 2A shows the results of the subtraction of the ACN features of spectrum b from the features of the octadecyl ligands in spectrum a. The subtraction was stopped at this point because the ν (C–CN) band had been nearly completely removed. In fact, it appears that slightly too much of this feature has been removed, since it looks as though two distorted bands are now present in this region (spectrum c). The ν_a (C–C) and ν_s $(C–C)_T$ features due to octadecyl ligands are now more clearly evident than they were in spectrum a, and the τ (CH_2) and δ_a $(CH_3)/\delta_{sci}$ (CH_2) bands are now the most prominent spectral features in spectrum c. Although the very prominent ν (C–CN) feature has been nearly completely subtracted, the weaker δ $(CH_3)_{CN}$ band is still present in spectrum c. The existence of the δ $(CH_3)_{CN}$ band, even after complete subtraction of the ν (C–CN) band seems to indicate that the ACN mobile phase is present in two different environments, bulk ACN and those ACN molecules associated with the stationary phase ligands. If the ACN was homogeneously distributed and in the same molecular environment, all of the mobile phase features should have decreased at the same relative rate upon subtraction. In support of this

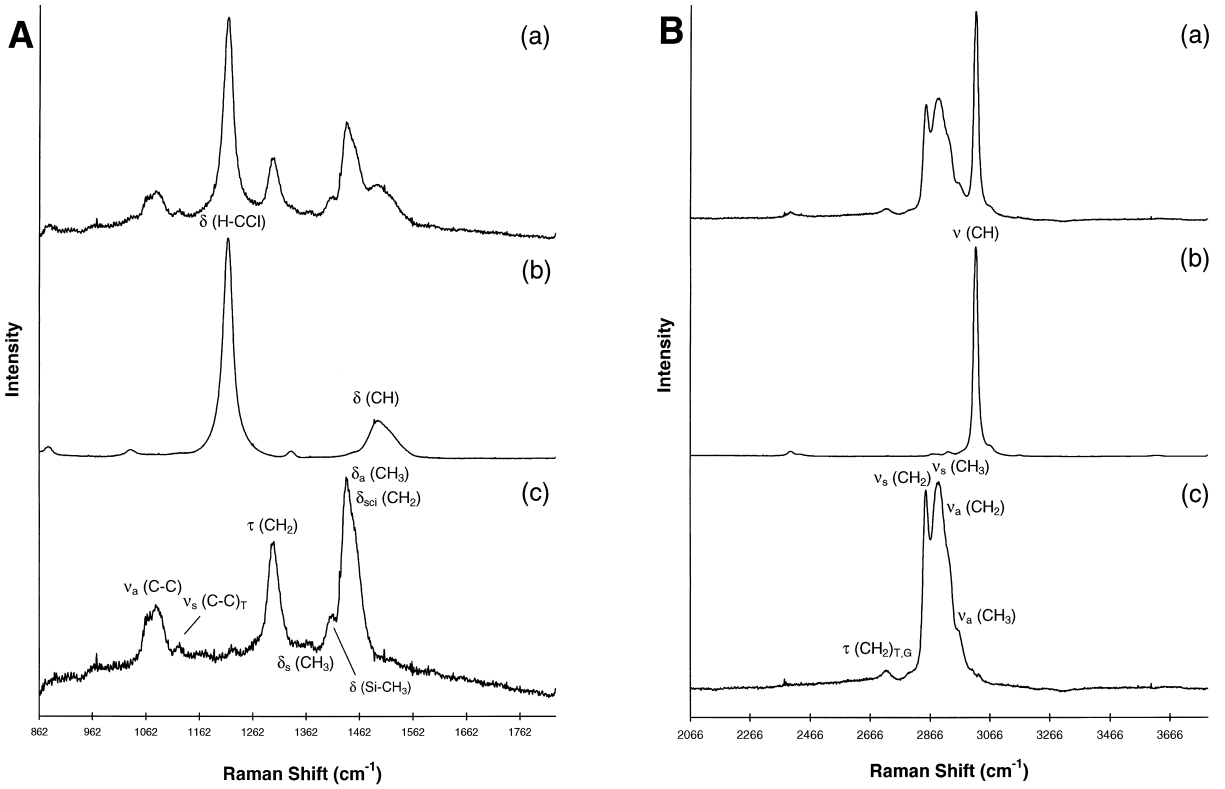

Fig. 4. (A) Comparison of the spectral features in the C–C stretching and C–H bending region due to the bonded ligands of the 3.52 μmol m^{-2} Microporasil C_{18} stationary phase at 35°C (a) in the presence and (c) absence of the spectral features due to the (b) chloroform mobile phase (1.0 ml min^{-1}). Spectral scaling factors: (a) ×4.893, (b) ×1, (c) ×9.350. (B) Same as (A), except that the spectral region is the C–H stretching region. Spectral scaling factors: (a) ×5.480, (b) ×1, (c) ×9.490.

conclusion, other studies [28,29,54–58] have found that the stationary phase ligands are enriched in the organic component of aqueous–organic mobile phase mixtures.

Ignoring the fact that the subtraction is already complete in the ν (C–CN) region (spectrum c of Fig. 2A), further subtraction of ACN within a more narrow spectral region (spectrum d) allows further removal of the δ $(CH_3)_{CN}$ band from the features due to the octadecylsilyl ligands of the stationary phase. Some residual intensity is still evident in the δ $(CH_3)_{CN}$ spectral region in spectrum d, but additional subtraction of ACN would have introduced anomalous negative features. An estimate of how much ACN is associated with the C_{18} stationary phase ligands can be obtained from the intensities observed for the δ $(CH_3)_{CN}$ band. The δ $(CH_3)_{CN}$ band of spectrum a has been reduced to about 23–27% of its original intensity in spectrum c, and has been further reduced to about 5.5–10% of its original intensity in spectrum d.

Although there is still some spectral intensity due to ACN in the δ $(CH_3)_{CN}$ region, the spectral features due to the octadecylsilyl ligands look very similar, regardless of whether the ligands were exposed to an aqueous mobile phase (spectrum c of Fig. 1A) or to an ACN mobile phase (spectrum d of Fig. 2A). The most obvious difference between these two spectra is that the octadecylsilyl features in the region between 1230 and 1600 cm^{-1} appear to be on top of a relatively broad background envelope of intensity in the case of the spectrum with ACN features removed (spectrum d of Fig. 2A).

In the high wavenumber region (Fig. 2B), ACN

(spectrum b) exhibits features at 2253, 2942 and 3002 cm^{-1} due to nitrile stretching [ν (CN)], and methyl symmetric [ν_s $(CH_3)_{CN}$] and asymmetric stretching [ν_a $(CH_3)_{CN}$], respectively. The ν (CN) and ν_s $(CH_3)_{CN}$ bands due to ACN are considerably more prominent than the ν_s (CH_2) and ν_s (CH_3) spectral features due to the octadecyl ligands that are also evident in spectrum a. Subtraction of ACN spectral features (spectrum b) from the octadecyl ligand features (spectrum a) in the high wavenumber region yields spectrum c of Fig. 2B. Subtraction of the ACN ν_s $(CH_3)_{CN}$ band slightly distorted the spectral features due to the bonded C_{18} ligands (spectrum c of Fig. 2B) in the region between approximately 2927 and 2959 cm^{-1}. Subtraction of ACN features was stopped at this point because further subtraction would have introduced more noticeable negative features in this region. The fact that ACN features are still evident in the ν (CN) and ν_a $(CH_3)_{CN}$ spectral regions again indicates that there are spectral differences between bulk and bonded ligand-associated ACN. Upon spectral subtraction, the intensities of the ν (CN) and ν_a $(CH_3)_{CN}$ bands of spectrum a have been reduced to 6% [ν (CN)] and 29% [ν_a $(CH_3)_{CN}$] of their original intensities in spectrum c. In agreement with the low wavenumber results, this appears to indicate that roughly about 10–25% of the ACN is associated with the bonded C_{18} ligands. This percentage is in qualitative agreement with the value of 30% of a neat MeOH mobile phase being associated with a C_{18} stationary phase, which can be calculated from results reported by Yonker et al. [28] for the volume of the mobile phase (0.782 ml), the volume of MeOH in the stationary phase (0.37 ml g^{-1} of stationary phase), and the amount of stationary phase (0.8948 g) in the column. Despite the distortion of the spectral region from about 2927 to 2959 cm^{-1}, and the incomplete subtraction of the ACN ν_a $(CH_3)_{CN}$ band, the spectral features due to the 18 bonded ligands that originated from the neat ACN mobile phase environment (spectrum c of Fig. 2B) are fairly comparable to the C_{18} bonded ligand features obtained from the aqueous environment (spectrum c of Fig. 1B).

3.1.3. Subtraction of methanol features

As in the case of ACN, there is considerable overlap between the spectral features due to the C_{18} bonded ligands and those of the methanol mobile phase. In the low wavenumber region (Fig. 3A), the carbon–oxygen stretching [ν (C–O)] band at 1034 cm^{-1} and the methyl bending [δ $(CH_3)_{OH}$] band at 1452 cm^{-1} due to MeOH (spectrum b) overlap the ν_a (C–C) and the δ_a $(CH_3)/\delta_{sci}$ (CH_2) spectral features of the C_{18} bonded ligands (spectrum a). Subtraction of the MeOH features (spectrum b) from the features due to the bonded C_{18} ligands (spectrum a) yields a relatively inadequate subtraction of MeOH features (spectrum c) in the low wavenumber region (Fig. 3A). Although the ν_s $(C–C)_T$, τ (CH_2), δ_s (CH_3), and δ $(Si–CH_3)$ spectral features due to the C_{18} ligands are clearly evident in spectrum c of Fig. 3A, the ν_a (C–C) and δ_a $(CH_3)/\delta_{sci}$ (CH_2) regions are clearly distorted by residual MeOH features, in comparison to similar regions obtained after removal of H_2O (spectrum c of Fig. 1A) and ACN (spectrum d of Fig. 2A) features.

Incomplete subtraction of methanol has resulted in a relatively broad region of spectral intensity from about 995 to 1050 cm^{-1} due to the partial overlap of the bonded octadecyl ν_a (C–C) band and the residual MeOH ν (C–O) band (spectrum c of Fig. 3A). In the region from about 1420 to 1530 cm^{-1}, incomplete subtraction of the MeOH δ $(CH_3)_{OH}$ band from the bonded C_{18} band due to the combination of δ_a (CH_3) and δ_{sci} (CH_2) yields a relatively broad feature encompassing this entire region. This C_{18}/residual MeOH band is considerably broader than the δ_a $(CH_3)/\delta_{sci}$ (CH_2) band observed after removal of either H_2O (spectrum c of Fig. 1A) or ACN (spectrum d of Fig. 2A) spectral features. In addition, the intensity of this C_{18}/residual MeOH band, relative to the τ (CH_2) band, is considerably more intense in comparison to the same spectral regions following the removal of either H_2O (spectrum c of Fig. 1A) or ACN (spectrum d of Fig. 2A) spectral features.

The inability to completely subtract the spectral features due to MeOH from the features due to the C_{18} bonded ligands again suggests that MeOH, like ACN, is present as both bulk solvent and as MeOH associated with the bonded C_{18} ligands of the stationary phase. Unfortunately, an estimate as to the amount of MeOH that is associated with the bonded C_{18} ligands is not readily achievable from the spectra, because MeOH, unlike ACN, does not have

distinctive spectral features, separate from those of the bonded C_{18} ligands, that are still present after subtraction.

In the high wavenumber region (Fig. 3B), the features due to the bonded C_{18} ligands are not even readily discernible from those due to MeOH (spectrum a). The ν_s $(CH_3)_{OH}$ and ν_a $(CH_3)_{OH}$ bands due to MeOH at 2835 and 2942 cm^{-1}, respectively (spectrum b), substantially overlap the C–H stretching features due to C_{18} bonded ligands (spectrum a). Even with such overlapping of spectral features, removal of MeOH solvent features (spectrum b) from the features due to the bonded phase ligands in the presence of MeOH (spectrum a) gives C_{18} ligand spectral features (spectrum c) that are very similar to the features observed following removal of either H_2O (spectrum c of Fig. 1B) or ACN (spectrum c of Fig. 2B) spectral features. The most notable difference between the C_{18} bonded ligand spectral features in the C–H stretching region obtained from MeOH, in comparison with those obtained from either H_2O or ACN, is that the ν_a (CH_3) region (spectrum c of Fig. 3B) has a more pronounced shoulder that extends out to about 3120 cm^{-1}, due to incomplete subtraction of MeOH. As was the case in the low wavenumber region (Fig. 3A), the incomplete subtraction of MeOH features from those of the bonded C_{18} ligands suggests that a portion of the MeOH is associated with the bonded ligands.

3.1.4. Subtraction of chloroform features

At this point, it does not appear that any drastic changes are occurring in the spectral features of the bonded C_{18} ligands upon exposure to the H_2O, ACN, and MeOH mobile phases, except for the presence of residual ACN and MeOH mobile phase features. Therefore, because chloroform is even less polar than either ACN or MeOH, the conformational changes of the bonded alkyl ligands in going from an aqueous environment to the less polar $CHCl_3$ environment should presumably be even more prominent than for similar transitions from an aqueous environment to either ACN or MeOH mobile phase environments. In addition, $CHCl_3$ is a convenient solvent from a spectroscopic point of view because its spectral features do not overlap those of the saturated hydrocarbon features due to the bonded C_{18} ligands (Fig. 4).

In the low wavenumber region (Fig. 4A), the chloro–methine deformation [δ (H–CCl)] of $CHCl_3$ at 1215 cm^{-1} (spectrum b) does not significantly overlap the C_{18} bonded phase spectral features (spectrum a), whereas the methine deformation [δ (C–H)] of $CHCl_3$ at 1497 cm^{-1} does partially overlap, but is of comparatively less intensity than the δ_a $(CH_3)/\delta_{sci}$ (CH_2) bonded phase features. Subtraction of the $CHCl_3$ features (spectrum b) from the features due to the bonded C_{18} ligands (spectrum a) yields C_{18} ligand spectral features (spectrum c) that are nearly identical to those obtained following the removal of H_2O spectral features (spectrum c of Fig. 1A), especially in the C–H bending region.

In the high wavenumber region (Fig. 4B), the methine stretching band of $CHCl_3$ [ν (C–H)] at 3019 cm^{-1} (spectrum b) only slightly overlaps the ν_a (CH_3) band of the C_{18} bonded ligands (spectrum a), leaving the majority of the C–H stretching features due to the bonded ligands clearly evident, even prior to subtraction of the $CHCl_3$ spectral features. Subtraction of the $CHCl_3$ spectral features (spectrum b) from the spectrum of the C_{18} bonded ligands in the presence of the $CHCl_3$ mobile phase (spectrum a) gives the spectral features due only to the bonded ligands (spectrum c). The C_{18} spectral features obtained in the C–H stretching region by removal of the $CHCl_3$ mobile phase features (spectrum c of Fig. 4B) are again similar to the features observed after removal of H_2O, ACN and MeOH. Comparison of the C_{18} features obtained from $CHCl_3$ (spectrum c of Fig. 4B) and from H_2O (spectrum c of Fig. 1B) does, however, indicate that the ν_s (CH_2) band is more prominent, relative to the ν_s (CH_3) band, for the C_{18} spectral features obtained from $CHCl_3$ than from H_2O.

3.2. Comparison of C_{18} features obtained from the different solvent environments

Superimposition of the C_{18} spectral features obtained from each of the different mobile phases allows the effects of the different mobile phases to be more readily examined. The spectral features due to the bonded ligands of the 3.52 μmol m^{-2} C_{18} stationary phase after subtraction of the spectral features due to each of the solvents are superimposed in Fig. 5. In the low wavenumber region (Fig. 5A),

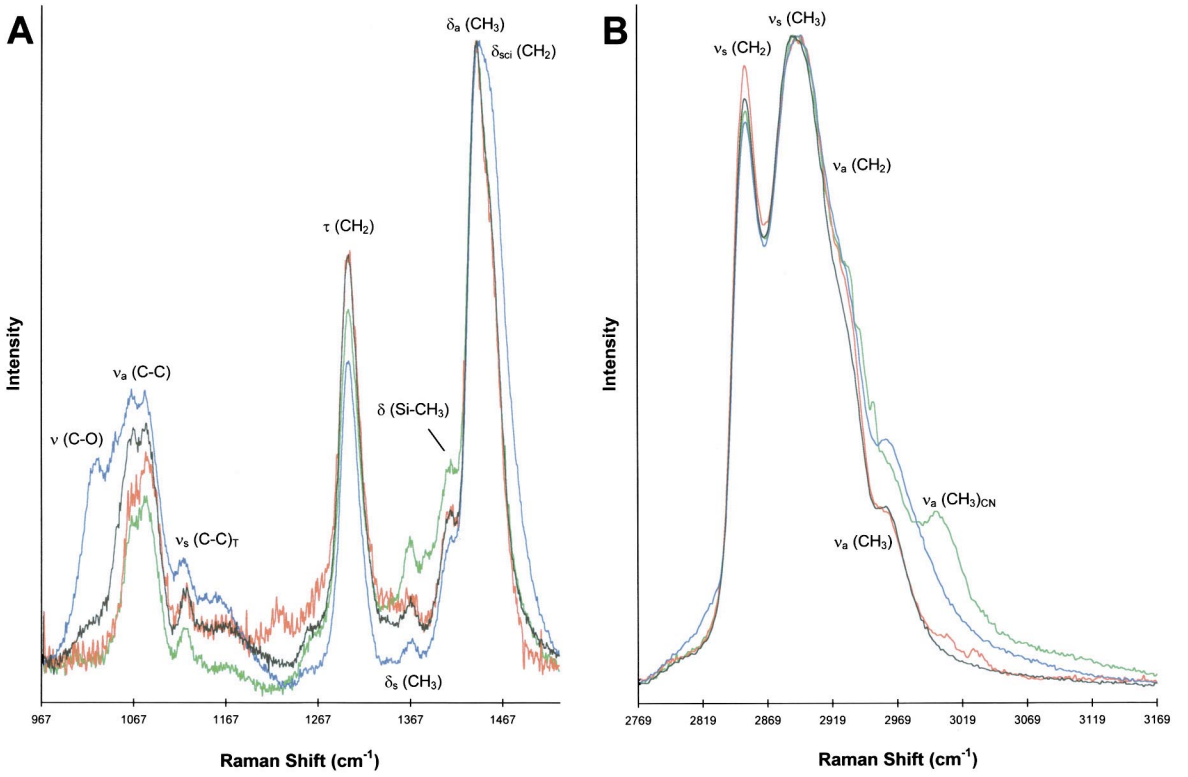

Fig. 5. (A) Comparison of the spectral features in the C–C stretching and C–H bending region due to the bonded ligands of the 3.52 μmol m^{-2} Microporasil C_{18} stationary phase at 35°C, after removal of methanol (blue, ×1), acetonitrile (green, ×1.047), water (black, ×1.311), and chloroform (red, ×2.738) mobile phase features. (B) Same as (A), except that the spectral region is the C–H stretching region. spectral scaling factors: methanol (×1), acetonitrile (×1.004), water (×1.350), chloroform (×1.761).

although the C–C stretching and C–H bending features due to the C_{18} bonded ligands are evident in each of the spectra, there are noticeable differences between the spectra obtained from the different solvent environments.

Some of the differences observed, particularly the different backgrounds of each spectrum, can be attributed at least in part to day-to-day experimental variations. There was typically a several day lag-time between each change in mobile phase solvent composition to allow the stationary phase ligands to be gradually, and fully equilibrated in each solvent prior to spectroscopic analysis. Thus the exact alignment of the laser, grating, fiber, and colunm have all changed at least slightly for each of the different solvents studied. Each of these parameters, as well as other possible contributing factors, could affect the overall appearance of the spectral backgrounds observed.

In particular, in the low wavenumber region (Fig. 5A), the spectral features obtained from $CHC1_3$ appear to be sitting on a concave background envelope; while the features obtained from MeOH appear to be sitting on a convex envelope; whereas the features obtained from ACN appear to be sitting on a concave envelope that covers a smaller spectral region from about 1236 to 1528 cm^{-1} and the features obtained from H_2O appear to be sitting on two concave envelopes covering the regions from 978 to 1210 cm^{-1} and from 1236 to 1528 cm^{-1}. Taking these background differences into account explains some of the apparent variability in peak

heights observed, particularly in the ν_a (C–C) and τ (CH_2) regions, for the different solvent environments.

Note that there is substantial agreement, in both band shapes and intensities, between the C_{18} spectral features obtained from H_2O and $CHCl_3$ environments, except for some minor variability in the ν_a (C–C) region. This region is particularly complex because not only are the ν_a (C–C) features relatively weak in comparison to the τ (CH_2) and δ_a (CH_3)/δ_{sci} (CH_2) bands, but there is also considerable overlap in this region with prominent spectral features due to the fused-silica of the fiber optic probe [46]. As noted in the experimental section, the features due to the fiber optic probe have already been subtracted from all spectra presented in this article.

The incomplete subtraction of MeOH features is obvious in Fig. 5A, especially in ν_a (C–C) and δ_a (CH_3)/δ_{sci} (CH_2) spectral regions. The incomplete removal of MeOH in the region from 1420 to 1528 cm^{-1} causes the relative intensity of the τ (CH_2) band to appear to be lower than for any other mobile phase, even after taking background differences into account. The C_{18} features obtained from ACN exhibit spectral intensity differences in the ν_a (C–C), τ (CH_2), δ_s (CH_3), and δ (Si–CH_3) regions, in comparison with those same features obtained from H_2O and $CHCl_3$, which may at least partially be explained in terms of differences in the background envelopes observed in these spectral regions. Also, some of the spectral intensity observed in the δ_s (CH_3) region probably arises from incomplete subtraction of the ACN δ $(CH_3)_{CN}$ band.

In the high wavenumber region (Fig. 5B), the overall appearance and shape of the ν_s (CH_2) and ν_s (CH_3) octadecyl features are in fairly good agreement for the different solvent environments. The incomplete subtraction of the ACN and MeOH mobile phase features are evident in the spectral region from about 2920 to 3169 cm^{-1}, especially in comparison to the features obtained from H_2O and $CHCl_3$. In the case of the C_{18} spectral features obtained from an ACN mobile phase environment, the residual ACN ν_a $(CH_3)_{CN}$ band is still evident at 2999 cm^{-1}. As noted previously, the ν_s (CH_2) band is more intense, relative to the ν_s (CH_3) band, for the octadecyl features obtained from $CHCl_3$ than for the same features obtained from H_2O. Additionally, in agreement with the observation that methylene symmetric stretching is more prominent in the $CHCl_3$ environment, the shoulder due to methylene asymmetric stretching is also more prominent when the bonded phase has been exposed to $CHCl_3$, in comparison to the effect of H_2O exposure. Also of note with regards to the features obtained from exposure to $CHCl_3$ is the slight increase in intensity, in comparison to the features obtained from H_2O, in the region between 2993 and 3041 cm^1, due to incomplete subtraction of the ν (CH) band of $CHCl_3$. Comparison of the relative intensities of the ν_s (CH_2) and ν_s (CH_3) bands appears to indicate that methylene symmetric stretching of the bonded ligands is sensitive to the solvent environment, and becomes decreasingly less prominent when the ligands have been exposed to $CHCl_3$>H_2O>ACN> and MeOH. However, the results obtained from ACN and MeOH in the methylene asymmetric stretching region appear to indicate that methylene asymmetric stretching of the bonded ligands is even more prevalent in these mobile phase environments than in either H_2O or $CHCl_3$. We do not yet know how to interpret these seemingly contradictory results in terms of ligand structure.

3.3. Preliminary discussion of solvent-induced ligand conformational changes

The close agreement between the C_{18} bonded ligand spectral features obtained after removal of H_2O solvent features and after removal of $CHCl_3$ solvent features seems to indicate that the bonded ligands do not undergo very drastic conformational changes, even with relatively drastic changes in solvent polarity. Although conclusions based on the results obtained from ACN and MeOH are more difficult because of the incomplete subtraction of solvent features in these cases, these results also appear to indicate that the changes in solvent polarity do not appear to induce drastic conformational changes in the bonded ligands.

Another possible explanation for the apparent lack of changes in the C_{18} spectral features with such drastic changes in solvent environments could be quite simply that Raman spectroscopy is just not sensitive to ligand conformational changes induced by different solvent environments. This explanation

does not appear to be feasible based on the changes observed in comparing the methylene stretching features obtained from H_2O and $CHCl_3$ environments, as previously discussed. Although it is difficult to assign specific ligand conformations based on these changes at present, these results may indicate that $CHCl_3$ is inducing some slight conformational changes, presumably to a slightly more ordered configuration according to the present theories of alkyl chain conformations under solvated conditions. In addition, the results presented in the following article [59] demonstrate that spectroscopic changes are observed under different solvated conditions as a function of temperature. Taken together, these results appear to indicate that, contrary to popular belief, the changes from a collapsed configuration under aqueous conditions to a more solvated and extended configuration under higher organic content mobile phase conditions does not occur. Apparently the changes are much more subtle.

From a spectroscopic standpoint, it is clearly easier to obtain the bonded phase spectral features if they are not obscured by the overlap of solvent spectral features, as is the case for H_2O and $CHCl_3$. Unfortunately, the spectral features of ACN and MeOH, which are more relevant solvents from a chromatographic standpoint than $CHCl_3$, considerably overlap the C_{18} bonded ligand spectral features making the subtraction of solvent features more difficult. Considering that Raman scattering is an inherently weak phenomenon and that alkyl ligands are particularly weak Raman scatterers [41,60], the quality of the spectra presented in this manuscript is quite good, especially since the bonded C_{18} ligands are only present in sub-monolayer coverages. Even with the subtraction difficulties encountered for the ACN and MeOH mobile phases, the spectroscopic results obtained are still informative. The quality of the bonded phase spectra obtained from ACN and MeOH solvent systems could be improved, however, by employing either deuterated solvents and conventional stationary phase ligands, and/or conventional solvents and various bonded ligands which have been deuterated at different points along the length of the carbon backbone. These deuterated systems would allow the presently overlapping bonded phase/solvent features to be more clearly resolved prior to spectral subtraction. Deuterated organic solvents would be particularly useful in investigating solute interactions in hydro–organic mobile phases. Standard, non-deuterated, ACN and MeOH were selected for these initial studies to keep the conditions as close to those used in RPLC as possible.

3.4. Effects of ligand bonding density in various mobile phase environments

A number of chromatographic studies have found that the density of ligands attached to the support surface can affect the outcome of RPLC separations [13,19,20,22]. Therefore, the effect of stationary phase ligand bonding density under various mobile phase conditions was investigated by Raman spectroscopy. The effects of the different mobile phase environments on the ligand spectral features of a 2.34 μmol m^{-2} Microporasil C_{18} stationary phase were compared to the ligand spectral features of the 3.52 μmol m^{-2} Microporasil C_{18} stationary phase under identical conditions.

As was observed previously [46], the relative intensities of the ligand spectral features obtained from aqueous mobile phases were nearly identical for both the 2.34 and 3.52 μmol m^{-2} Microporasil C_{18} stationary phases. A linear dependence between the spectral band intensity of the C_{18} bonded ligands and the number of stationary phase ligands attached to the support surface was observed for the τ (CH_2), δ_a (CH_3)/δ_{sci} (CH_2), ν_s (CH_2), and ν_s (CH_3) spectral features, following subtraction of the spectral features due to the H_2O mobile phases employed [46].

Due to the fact that there are fewer C_{18} ligands contributing to the bonded ligand spectral intensity for the 2.34 μmol m^{-2} phase, compared to the 3.52 μmol m^{-2} phase, subtraction of solvent features, for both acetonitrile and methanol mobile phases, was even more difficult than for the 3.52 μmol m^{-2} stationary phase (Figs. 2, 3 and 5). The bonded phase spectral features for the 2.34 μmol m^{-2} C_{18} stationary phase were even more obscured by residual solvent features. However, similar bonded ligand spectral features were still observed for both the 2.34 and 3.52 μmol m^{-2} Microporasil C_{18} stationary phases following subtraction of either the acetonitrile or the methanol mobile phase spectral features. Bonded ligand spectral feature differences

were observed as a function of bonding density, however, for the two stationary phases exposed to chloroform (Fig. 6).

As has already been discussed, the features due to $CHCl_3$, unlike those of ACN and MeOH, do not overlap the C_{18} bonded ligand spectral features. Therefore, the spectral differences observed for the 2.34 and the 3.52 μmol m^{-2} C_{18} stationary phases upon exposure to the $CHCl_3$ environment (Fig. 6) are due to changes of the stationary phase ligands, and not to incomplete removal of $CHCl_3$ spectral features. The small spectral differences observed in the low wavenumber region (Fig. 6A) for these two stationary phases mainly arise from background effects. The spectrum of the 2.34 μmol m^{-2} C_{18} phase is considerably more noisy than that of the 3.52 μmol m^{-2} C_{18} phase, due to fewer ligands contributing to the bonded ligand spectral intensity for the 2.34 μmol m^{-2} C_{18} phase. Additionally, although the $CHCl_3$ and C_{18} spectral features do not overlap in this spectral region, a residual $CHCl_3$ feature is still evident at about 1224 cm^{-1} for the 2.34 μmol m^{-2} C_{18} phase. Except for these minor differences, the spectral features due to the 2.34 and the 3.52 μmol m^{-2} C_{18} stationary phases in the low wavenumber region are essentially identical. In the high wavenumber region (Fig. 6B) however, not only is the peak maximum of the ν_s (CH_3) band shifted from 2892.7 cm^{-1} for 3.52 μmol m^{-2} C_{18} phase to 2895.8 cm^{-1} for the 2.34 μmol m^{-2} C_{18} phase, but methylene stretching is more prominent for the 2.34 μmol m^{-2} C_{18} phase as evidenced by the appearance of an actual shoulder in the ν_a (CH_2) region. The $CHCl_3$ environment is therefore affecting the ligands of the 2.34 μmol m^{-2} C_{18} stationary phase differently than the aqueous environment, in

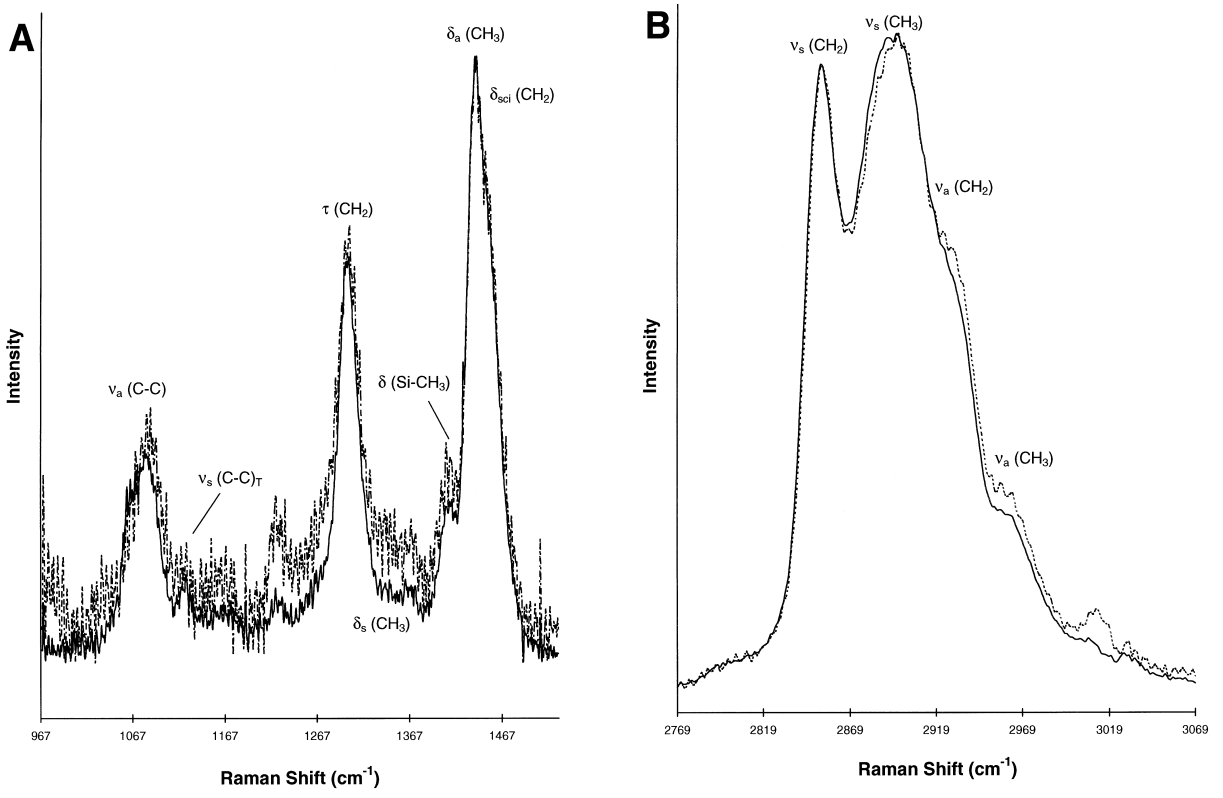

Fig. 6. (A) Comparison of the spectral features in the C–C stretching and C–H bending region due to the bonded ligands of the 2.34 μmol m^{-2} (– – –, ×1.008) Microporasil C_{18} and the 3.52 μmol m^{-2} (———, ×1) Microporasil C_{18} stationary phases at 35°C, with the spectral features due to the chloroform mobile phase removed (as in spectrum C of Fig. 4A). (B) Same as (A), except that the spectral region is the C–H stretching region. spectral scaling factors: 2.34 μmol m^{-2} C_{18} (×1.199), 3.52 μmol m^{-2} C_{18} (×1).

which no increase in asymmetric methylene stretching was observed for the same stationary phase.

4. Summary and conclusions

The feasibility of using Raman spectroscopy to examine stationary phase–mobile phase interactions has been demonstrated. Both acetonitrile and methanol have been shown to associate with the stationary phase ligands, and it was estimated that about 10–25% of the neat acetonitrile mobile phase molecules were associated with the ligands of the 3.52 μmol m^{-2} Microporasil C_{18} stationary phase. The effects of the exposure of the bonded C_{18} ligands to different solvents were shown to be accessible to characterization by Raman spectroscopy.

The drastic solvent-induced conformational changes of the bonded C_{18} ligands, from a collapsed state in the presence of the polar aqueous mobile phase to an extended 'brushlike' state in less polar organic mobile phases, was not observed by Raman spectroscopy. Such conformational changes would have been indicated by significant spectral changes in the carbon–carbon stretching region for the bonded phase ligands. No dramatic changes in the carbon– carbon stretching region were observed with mobile phase changes, although, as is shown in the subsequent article [59], the temperature effects on the C_{18} bonded ligand spectral features in this region are significant. Nonetheless, more subtle solvent-induced conformational changes were observed, as evidenced by the differences in methylene stretching of the bonded C_{18} ligands in aqueous and chloroform mobile phase environments. Bonded ligand methylene stretching was observed to be more prominent in chloroform than in water, and was observed to be more prominent for the lower bonding density stationary phase upon exposure to chloroform.

Interpretation of the effects of acetonitrile and methanol on the conformational behavior of the bonded C_{18} ligands was complicated by the incomplete subtraction of the solvent features. The C_{18} ligand spectral features obtained from acetonitrile and methanol, as with those obtained from water and chloroform, do not support the hypothesis that the stationary phase ligands collapse and elongate with changes in mobile phase composition. However, more subtle solvent-induced changes were not readily discernable in acetonitrile and methanol, due to the overlapping of bonded ligand and solvent spectral features. The use of deuterated acetonitrile and methanol solvents would provide more information about the effects of these solvents on the orientations of the C_{18} ligands.

Acknowledgements

The technical expertise of Mr. Keith Collins for assistance in the design and manufacture of the Raman–LC columns and the Raman liquid–solid cells employed in this study is gratefully acknowledged. The synthesis of the Microporasil C_{18} stationary phases by Ms. Jessica Wysocki is also gratefully acknowledged. The authors are grateful for support of this work by NIH GM-48561, and JGD is grateful to Merck Research Laboratories for continued support of our work.

References

[1] C.A. Doyle, J.G. Dorsey, in: E. Katz, R. Eksteen, P. Schoenmakers, N. Miller (Eds.), The Handbook of Liquid Chromatography, Marcel Dekker, New York, 1998, p. 293.
[2] B.L. Karger, J.R. Gant, A. Hartkopf, P.H. Weiner, J. Chromatogr. 128 (1976) 65.
[3] C. Horváth, W. Melander, I. Molnár, J. Chromatogr. 125 (1976) 129.
[4] C. Horváth, W. Melander, J. Chromatogr. Sci. 15 (1977) 393.
[5] W. Melander, C. Horváth, in: C. Horváth (Ed.), High-performance Liquid Chromatography — Advances and Perspectives, Vol. 2, Academic Press, New York, 1980, p. 201.
[6] S.A. Wise, W.J. Bonnet, F.R. Guenther, W.E. May, J. Chromatogr. Sci. 19 (1981) 457.
[7] S.A. Wise, W.E. May, Anal. Chem. 55 (1983) 1479.
[8] L.C. Sander, S.A. Wise, Anal. Chem. 56 (1984) 504.
[9] S.A. Wise, L.C. Sander, J. High Resolut. Chromatogr. Chromatogr. Commun. 8 (1985) 248.
[10] L.C. Sander, S.A. Wise, J. High Resolut. Chromatogr. Chromatogr. Commun. 11 (1988) 383.
[11] L.C. Sander, J. Chromatogr. Sci. 26 (1988) 380.
[12] L.C. Sander, S.A. Wise, LC·GC 8 (1990) 378.
[13] K.B. Sentell, J.G. Dorsey, J. Chromatogr. 461 (1989) 193.
[14] L.C. Sander, S.A. Wise, J. Chromatogr. 656 (1993) 335.
[15] M.C. Hennion, C. Picard, M. Caude, J. Chromatogr. 166 (1978) 21.
[16] G.E. Berendsen, L. de Galan, J. Chromatogr. 196 (1980) 21.

[17] A. Tchapla, H. Colin, G. Guiochon, Anal. Chem. 56 (1984) 621.
[18] L.C. Sander, S.A. Wise, Anal. Chem. 59 (1987) 2309.
[19] K.D. Lork, K.K. Unger, Chromatographia 26 (1988) 115.
[20] A. Tchapla, S. Heron, J. Chromatogr. A 684 (1994) 175.
[21] L.C. Sander, K.E. Sharpless, N.E. Craft, S.A. Wise, Anal. Chem. 66 (1994) 1667.
[22] K.B. Sentell, J.G. Dorsey, Anal. Chem. 61 (1989) 930.
[23] R.P.W. Scott, P. Kucera, J. Chromatogr. 142 (1977) 213.
[24] C.H. Löchmuller, D.R. Wilder, J. Chromatogr. Sci. 17 (1979) 574.
[25] R.P.W. Scott, C.F. Simpson, J. Chromatogr. 197 (1980) 11.
[26] R.K. Gilpin, J.A. Squires, J. Chromatogr. Sci. 19 (1981) 195.
[27] R.K. Gilpin, M.E. Gangoda, A.E. Krishen, J. Chromatogr. Sci. 20 (1982) 345.
[28] C.R. Yonker, T.A. Zwier, M.F. Burke, J. Chromatogr. 241 (1982) 257.
[29] C.R. Yonker, T.A. Zwier, M.F. Burke, J. Chromatogr. 241 (1982) 269.
[30] D.E. Martire, R.E. Boehm, J. Phys. Chem. 87 (1983) 1045.
[31] C.H. Lochmüller, M.L. Hunnicutt, J.F. Mullaney, J. Phys. Chem. 89 (1985) 5770.
[32] M. Hanson, K.K. Unger, J. Schmid, K. Albert, B. Bayer, Anal. Chem. 65 (1993) 2249.
[33] R.K. Gilpin, J. Chromatogr. A 656 (1993) 217.
[34] T.C. Schunk, M.F. Burke, J. Chromatogr. 656 (1993) 289.
[35] Z. Li, S.C. Rutan, S. Dong, Anal. Chem. 68 (1996) 124.
[36] K.B. Sentell, J. Chromatogr. A 656 (1993) 231.
[37] K.B. Sentell, D.M. Bliesner, S.T. Shearer, in: J.J. Pesek, I.E. Leigh (Eds.), Chemically Modified Surfaces, Royal Society of Chemistry, Cambridge, 1994, p. 190.
[38] S.C. Rutan, J.M. Harris, J. Chromatogr. A 656 (1993) 197.
[39] L.C. Sander, J.B. Callis, L.R. Field, Anal. Chem. 55 (1983) 1068.
[40] P. Guyot-Sionnest, R. Superfine, J.H. Hunt, Y.R. Shen, Chem. Phys. Lett. 144 (1988) 1.
[41] W.R. Thompson, J.E. Pemberton, Anal. Chem. 66 (1994) 3362.
[42] S.J. Klatte, T.L. Beck, J. Phys. Chem. 99 (1995) 16024.
[43] S.J. Klatte, T.L. Beck, J. Phys. Chem. 100 (1995) 5931.
[44] M.E. Montgomery Jr., M.A. Green, M.J. Wirth, Anal. Chem. 64 (1992) 1170.
[45] L.R. Snyder, J.J. Kirkland, Introduction to Modern Liquid Chromatography, 2nd ed., Wiley, New York, 1979.
[46] C.A. Doyle, T.J. Vickers, C.K. Mann, J.G. Dorsey, J. Chromatogr. A 779 (1997) 91.
[47] D.R. Lombardi, C. Wang, B. Sun, A.W. Fountain III, T.J. Vickers, C.K. Mann, F.R. Reich, J.G. Douglas, B.A. Crawford, F.L. Kohlasch, Appl. Spectrosc. 48 (1994) 875.
[48] C.K. Chong, C. Shen, Y. Fong, J. Zhu, F. Yan, S. Brush, C.K. Mann, T.J. Vickers, Vib. Spectrosc. 3 (1992) 35.
[49] K.B. Sentell, K.W. Barnes, J.G. Dorsey, J. Chromatogr. 455 (1988) 95.
[50] J.N. Kinkel, K.K. Unger, J. Chromatogr. 316 (1984) 193.
[51] R. Callender, H. Deng, Annu. Rev. Biophys. Biomol. Struct. 23 (1994) 215.
[52] D. Lin-Vien, N.B. Colthup, W.G. Fateley, J.G. Grasselli, The Handbook of Infrared and Raman Characteristic Frequencies of Organic Molecules, Academic Press, New York, 1991.
[53] R.M. Silverstein, G.C. Bassler, T.C. Morrill, Spectrometric Identification of Organic Compounds, 5th ed, Wiley, New York, 1991.
[54] A. Tilly-Melin, Y. Askemark, K.-G. Wahlund, G. Schill, Anal. Chem. 51 (1979) 976.
[55] R.M. McCormick, B.L. Karger, Anal. Chem. 52 (1980) 2249.
[56] E.H. Slaats, W. Markovski, J. Fekete, H. Poppe, J. Chromatogr. 207 (1981) 299.
[57] N.L. Ha, J. Ungváral, E. Kováts, Anal. Chem. 54 (1982) 2410.
[58] A. Alvarez-Zepeda, D.E. Martire, J. Chromatogr. 550 (1991) 285.
[59] C.A. Doyle, T.J. Vickers, C.K. Mann, J.G. Dorsey, J. Chromatogr. A, in press.
[60] D.J. Gardiner, in: D.J. Gardiner, P.R. Graves (Eds.), Practical Raman Spectroscopy, Springer-Verlag, New York, 1989, p. 1.